Asymptotic Model of the Flow in Metallic and Elastomeric Progressive Cavity Pump

S. F. A. Andrade, selmafaa@petrobras.com.br
J. V. Valério, jujuvianna@gmail.com
M. S. Carvalho, msc@puc-rio.br
Departamento de Engenharia Mecânica, PUC-Rio, R. Mq.S.Vicente 225, Rio de Janeiro, 22453-900, Brasil

Abstract. *Progressive Cavity Pump (PCP) is one of the most used technologies for transporting different fluid-like materials, from sandy crude oil to waste sludge. In its simplest form, it consists of a single threaded screw (rotor) turning inside a double threaded nut (stator), forming cavities separated by seal lines. The stator can be metallic or covered with an elastomeric layer. This apparently simple mechanism produces a more-or-less pulsation-free positive displacement flow, without the need for valves, based on the movement of the cavities from the suction to the discharge, as the rotor turns inside the stator. PCPs are largely used in the oil industry because of their ability to pump liquids with high solid contents, high efficiency with high viscosity liquids, unique design, and simple installation and operation. The performance of a PCP is a function of the rotor diameter and eccentricity, stator diameter and pitch, the number of stages, and rubber cover properties, in the case of elastomeric PCPs. Oil production completions with PCPs are generally designed using characteristics pump curves provided by manufacturers. However, several variables, such as viscosity, solid and gas contents - not taken into account in these curves - can affect the volumetric efficiency of both metallic and elastomeric stator pumps. The analysis of pump performance at oil field conditions is the main goal of research on PCPs. The pressure drop - flow rate relationship of a PCP depends strongly on the pressure driven back flow between two consecutive cavities. Many models have been presented to try to describe this back flow, commonly referred to as slip flow. Only recently, a complete three-dimensional, transient model of the flow has been presented. The solution is extremely complex and computationally expensive mainly because of the 3-D character of the flow, the complexity of the geometry and mesh motion to follow the rotor movement. The results agree well with experimental data, however the use of the model for testing different operating conditions and pump designs is limited, since the time to compute the flow at each conditions is extremely large (over one week). The problem becomes even more complex in the case of elastomeric stator. Realizing that there is a large ratio of length scales in the region between consecutive cavities, we propose an asymptotic model to describe the flow inside PCPs. The model reduces the three-dimensional Navier-Stokes equation to a two-dimensional Poisson's equation for the pressure field inside the pump. At each time step, it was solved by a second-order finite difference scheme. The results obtained agree very well (discrepancy less than 5%) with the complete 3D model, however the computational time required is approximately 100 times smaller. The asymptotic model will make it simpler to extend the model to PCPs with deformable stator, multiphase flow and different geometries.*

Keywords: *Progressive Cavity Pump; Lubrication Approximation; Numerical Model*

1. INTRODUCTION

Almost every fluid-like material can be pumped with Progressive Cavity Pumps. Since the pumping principle conceived by the french engineer René Moineau [1] in the 1930's, a large number of different industrial applications puts this positive displacement pump in the group of the most used technologies for moving fluids, from sandy crude oil to waste sludge. Progressive Cavity Pumps (PCP) in their simplest form consist of a single threaded screw (rotor), turning inside a double threaded nut (stator), forming consecutive cavities separated by seal lines. This simple configuration belongs to the singlelobe category of PCP. More complex geometries with a large number of lobes are also used, and any combination is possible as long as the stator has one more lead than the rotor. The first generation of PCP's had a metallic rotor and stator, forming rigid moving cavities in the space between the two surfaces. The following generations presented a rubber covered stator, which is common nowadays. The deformable stator creates a compression fit with the rotor, in contrast with the metallic pump where there is a small clearance leading to a larger leakage between consecutive cavities. Considering that deformable stators have operational limitations, related with temperature and mechanical resistance of the elastomers, metallic PCPs have great application opportunity, and it has been recognized by the oil industry that this pump could become an important technological alternative for heavy oil production. This apparently simple mechanism produces an almost pulsation-free positive displacement flow, without the need for valves, based on the movement of the cavities from the suction to the discharge ends of the pump as the rotor turns inside the stator. The volumetric flow delivered by a PCP at a constant rotor speed and pressure difference depends on three design features: rotor diameter, rotor eccentricity and stator pitch. The pump pressure rating depends on the number of stages. The peculiar characteristic of PCP is the occurrence of back flow, also denominated slip flow, derived from non perfectly sealed cavities.

Due to their unique design and principle of operation, PCP systems provide many benefits in oilfield applications, such as high solid content tolerance, best efficiency with high viscosity fluids, simple installation and operation. Oil production

with PCP is generally designed over the knowledge of characteristic pump curves provided by manufacturer, but several variables can affect and change the volumetric efficiency of both metallic and elastomeric stator pumps. It is common knowledge that the characteristic curves change significantly with liquid viscosity and gas content, therefore pump curves provided manufacturers usually do not represent the real pump performance at down hole conditions. Moreover, in order to design PCPs that can be operated at extreme conditions, it is important to understand the effect of each geometric design parameter on the pump performance. These are the main reasons behind research efforts dedicated to study the flow inside PCPs.

The performance of PCPs is a function of volumetric pump displacement and the slip flow ie, the backward flow between consecutive cavities due to the adverse pressure gradient along the pump. The limitation of simple models on predicting pump performance is related to the difficulties in calculating the internal back flow. For any type of stator, rigid or deformable, slippage is a function of the fluid characteristics, the differential pressure, the components dimensions and the kinematics. In the case of elastomeric stators the problem become even more complex, because the geometry of the flow channel becomes a function of the pressure field.

Olivet et al., (2002) [2] performed an experimental study and obtained characteristic curves and instantaneous pressure profiles along metal to metal pumps for single- and two-phase flow conditions.

The first and simplest numerical model to describe the flow inside the PCP was presented by Moineau (1930) [1] and is based on calculating the back flow across the pump, considering a Hagen-Poiseuille flow in the sealing lines, which is subtracted from the volume displaced by the rotating rotor, giving the volumetric flow rate. As the differential pressure across the pump rises, so does the slippage, and the relation between differential pressure and net volumetric flow pumped, can be calculated. Since the slippage gap area is not clearly defined, the model is able to describe the qualitative behavior, but it is not accurate.

The volumetric displacement associate with the rotor movement can be easily calculated from pump components geometry, but calculating a internal slip is not a trivial problem. In order to improve Moineau's model, Gamboa and Olivet (2003) [3] have modeled the slip as the superposition of two different mechanism: one due to the rotor's movement and other due to the differential pressure between two cavities. However, limitations were recognized and the model was not able to fit experimental data.

Only recently, a complete three-dimensional, transient model of the flow inside the cavities of a PCP has been presented (Paladino et al. (2008) [4]). The numerical solution obtained with a commercial CFD software is extremely complex and computationally expensive, mainly because of the transient and 3-D character of the flow, the complexity of the geometry and the necessary mesh motion to follow the rotor movement. The results agree well with experimental data, however the use of the model for testing different operating conditions and pump designs is limited, since the time to compute the flow at a single operating condition was over one week. Therefore, the time required to produce an entire pump performance curve would be enormous.

Realizing that the region that defines the flow rate - pressure drop relationship is the small clearance between the moving rotor and the stator, where the slip flow occurs, and that the ratio of length scale in this region is very hight, we propose an asymptotic model to describe the flow inside PCPs. The proposed model reduces the three-dimensional transient Navier-Stokes equation to a quasi-steady state two-dimensional Poisson's equation for the pressure field inside the pump.

This is the same idea behind simplified models of the flow in screw extruder - see Li and Hsieh (1994) [5] and Shuresh et. al (2008) [6]. The simplified models for extruder can predict the qualitative behavior, but they are still not accurate enough to use as a design tool, mainly because of the geometric and kinematic simplifications used. One of the hypothesis is to neglect the curvature effect of the cross section, and to describe the geometry of the flow region using cartesian coordinates. Pina and Carvalho (2006), [7] presented an lubrication approximation model in cylindrical coordinates to describe the flow in annular space with varying eccentricity and showed that neglecting he curvature effect can greatly compromise the accuracy of the model.

The objective of this work is to develop an asymptotic model for the flow inside a metallic (rigid) singlelobe progressive cavity pump. The cross section is parameterized using cylindrical coordinates and there is no simplified assumption of the geometry and kinematics of the rotor. The resulting 2D equation for the pressure field at each time step was discretized with a second order finite difference approximation. The model was used to obtain predictions of the pump performance curve as a function of rotor speed, liquid properties and pump geometry.

The results obtained agree very well (discrepancy less than 5%) with the complete 3D model, but the computational time required was approximately 1000 times smaller.

2. MATHEMATICAL MODELLING

The flow inside the pump cavitied is governed by the Navier-Stokes and continuity equations, which in cylindrical coordinates are:

$$\frac{1}{r}\frac{\partial rv}{\partial r}+\frac{1}{r}\frac{\partial w}{\partial \theta}+\frac{\partial u}{\partial z}=0,$$

$$\rho\left(\frac{\partial u}{\partial t}+u\frac{\partial u}{\partial z}+v\frac{\partial u}{\partial r}+\frac{w}{r}\frac{\partial u}{\partial \theta}\right)=\rho g_z-\frac{\partial p}{\partial z}+\mu\left\{\frac{1}{r}\frac{\partial}{\partial r}\left(r\frac{\partial u}{\partial r}\right)+\frac{1}{r^2}\frac{\partial^2 u}{\partial \theta^2}+\frac{\partial^2 u}{\partial z^2}\right\},$$

$$\rho\left(\frac{\partial v}{\partial t}+v\frac{\partial v}{\partial r}+u\frac{\partial v}{\partial z}+\frac{w}{r}\frac{\partial v}{\partial \theta}-\frac{w^2}{r}\right)=\rho g_r-\frac{\partial p}{\partial r}+\quad\mu\left\{\frac{\partial}{\partial r}\left(\frac{1}{r}\frac{\partial}{\partial r}(rv)\right)+\frac{1}{r^2}\frac{\partial^2 v}{\partial \theta^2}-\frac{2}{r^2}\frac{\partial w}{\partial \theta}+\frac{\partial^2 v}{\partial z^2}\right\},$$

$$\rho\left(\frac{\partial w}{\partial t}+v\frac{\partial w}{\partial r}+u\frac{\partial w}{\partial z}+\frac{w}{r}\frac{\partial w}{\partial \theta}-\frac{vw}{r}\right)=\rho g_\theta-\frac{1}{r}\frac{\partial p}{\partial \theta}+\mu\left\{\frac{\partial}{\partial r}\left(\frac{1}{r}\frac{\partial (rw)}{\partial r}\right)+\frac{1}{r^2}\frac{\partial^2 w}{\partial \theta^2}-\frac{2}{r^2}\frac{\partial v}{\partial \theta}+\frac{\partial^2 w}{\partial z^2}\right\}.$$

where u, v, and w are the axial, radial, and tangential velocity components. To avoid solving the system of coupled three-dimensional differential equations, dimensional analysis is used to eliminate some of the terms of the equations. The procedure used here is generally known as lubrication approximation.

The clearance between the rotor and stator is much smaller than the radius or length of the pump: $F=(R_o-R_r)\ll R_o\sim R_r\sim L$, as shown in the figure 1. Using continuity equation, it can be shown that the main flow is in the axial direction, the velocity component in the radial direction is much smaller than in the other two, i.e., $u, w \gg v$. Moreover, the variation of the velocity components in the axial and azimuthal directions are much smaller than those in the radial direction. Thus, the derivatives with respect to the radial direction are much larger than the others

$$\frac{\partial^2 u}{\partial r^2}\gg\frac{\partial^2 u}{\partial z^2},\frac{\partial^2 u}{\partial \theta^2}\quad\text{and}\quad\frac{\partial^2 w}{\partial r^2}\gg\frac{\partial^2 w}{\partial z^2},\frac{\partial^2 w}{\partial \theta^2}$$

By applying dimensional analysis the appropriate terms of the Navier-Stokes transient equations can be neglected and the system of differential equations becomes:

$$0=-\frac{\partial p}{\partial z}+\mu\left[\frac{1}{r}\frac{\partial}{\partial r}\left(r\frac{\partial u}{\partial r}\right)\right],\qquad 0=-\frac{\partial p}{\partial r},\qquad 0=-\frac{1}{r}\frac{\partial p}{\partial \theta}+\mu\left[\frac{\partial}{\partial r}\left(\frac{1}{r}\frac{\partial (rw)}{\partial r}\right)\right]. \tag{1}$$

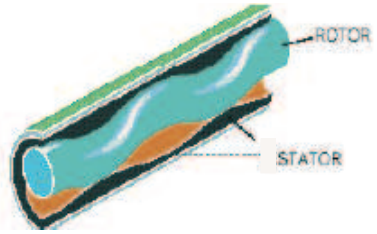

Figure 1. Components of PCP

Since the pressure is not a function of r, the velocities u and w can be analytically integrated in the radius direction in terms of the pressure:

$$u=\left(\frac{\partial p}{\partial z}-\rho g\right)\frac{1}{4\mu}r^2+c_1\ln r+c_2;\quad w=\frac{1}{2\mu}\frac{\partial p}{\partial \theta}\left(\ln r-\frac{1}{2}\right)+\frac{c_3}{2}r+\frac{c_4}{r}; \tag{2}$$

where c_1, c_2, c_3, c_4 are constants calculated based on the boundary conditions.

2.1 Pump Geometry and Integral Limits

The movement of the fluid inside the pump is caused by the single-threaded helical rotor rolling eccentrically inside a helical double-threaded stator. As the stator has a pitch length twice as long compared to the rotor, the fluid is trapped in consecutive quasi-sealed cavities. These cavities follow each other and produce a almost pulsation-free, positive displacement flow, figure 2.

The flow displacement inside of a PCP depends on three design features: Rotor radius (R_r), eccentricity (E) and stator pitch (P_{st}). Note, in figure 3, that the center of the cross section of the rotor is not the center of mass of the rotor (center of the rotor's helix) due to its helical nature. And the distance from the center of the rotor's helix and the center of the stator defines the eccentricity(E).

Our coordinate center lies on the center of the cross section of the rotor (C_r), therefore in a cross section of the pump it translates as shown in the figure 4. Eventhough the velocity component in the radius direction, v, is much smaller compared to the others, in the boundary condition v is considered, because of the pump kinematic. To describe the

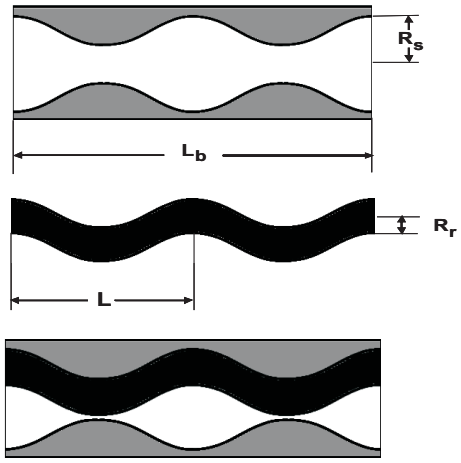

Figure 2. PCP longitudinal section

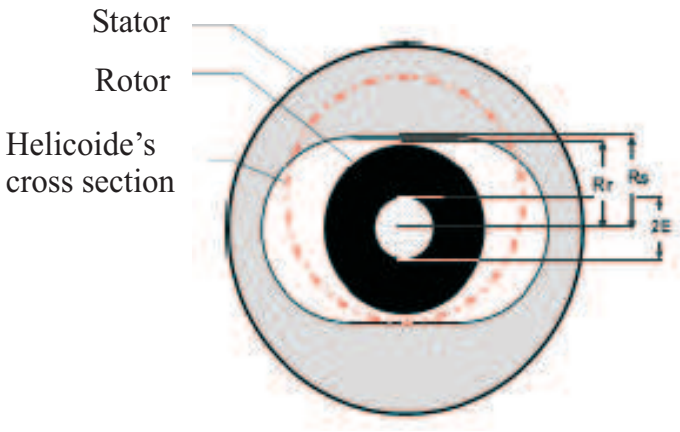

Figure 3. PCP's cross section.

geometry of the region where the fluid flows inside the pump, the position of the internal radius of the stator has to be derived as a equation of θ and z, $R_o(\theta, z)$. The cross section of the flow region varies from the rotor radius (R_r), which in our coordinate system is constant, to the internal radius of the stator ($R_o(\theta, z)$).

Figure 4. Rotation and translation of the rotor.

Some important variables used to describe this geometry, $R_o(\theta, z)$, are shown in figures 5 - 6 and defined below: $\Theta_S = \dfrac{2\pi z}{P_{st}} = \dfrac{\pi z}{P_r}$ is the angle between an horizontal axis from the rotor center to a central line of the stator; P_{st} and P_r are the stator and rotor piches; $d_{CSR} = \overline{C_s C_r} = 2E\cos(\Omega t - \Theta_S)$, so $-2E \leq \mathrm{d_{CSR}} \leq 2\mathrm{E}$ is the distance between the centers of the rotor and stator;
$\alpha_1 = \arctan\left(\dfrac{R_s}{2E - d_{CSR}}\right)$ and $\alpha_2 = \arctan\left(\dfrac{R_s}{2E + d_{CSR}}\right)$ are the angles between the central rotor line and the segments: $\overline{C_r A}$ to $\overline{C_r A'}$ and $\overline{C_r B}$ to $\overline{C_r B'}$, respectively.

We divided the region where the fluid flows in a cross section in four parts, as shown in figure 6. Each part of the region is represented by a function. The functions that describe $R_o(\theta, z)$ are written in the table 1, which also shows the

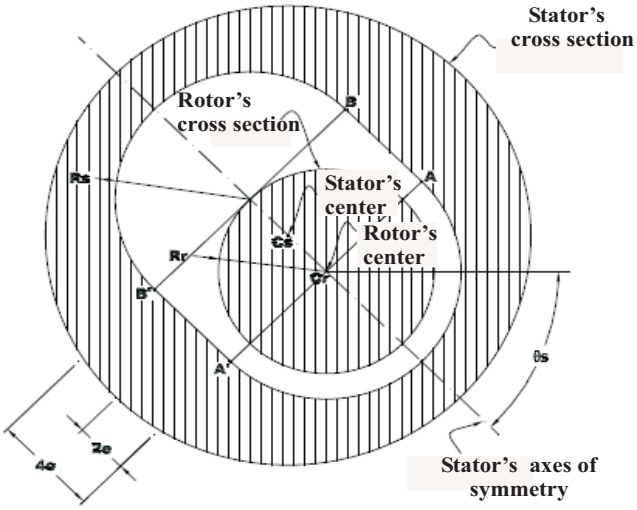

Figure 5. Geometrical elements of the PCP's cross section

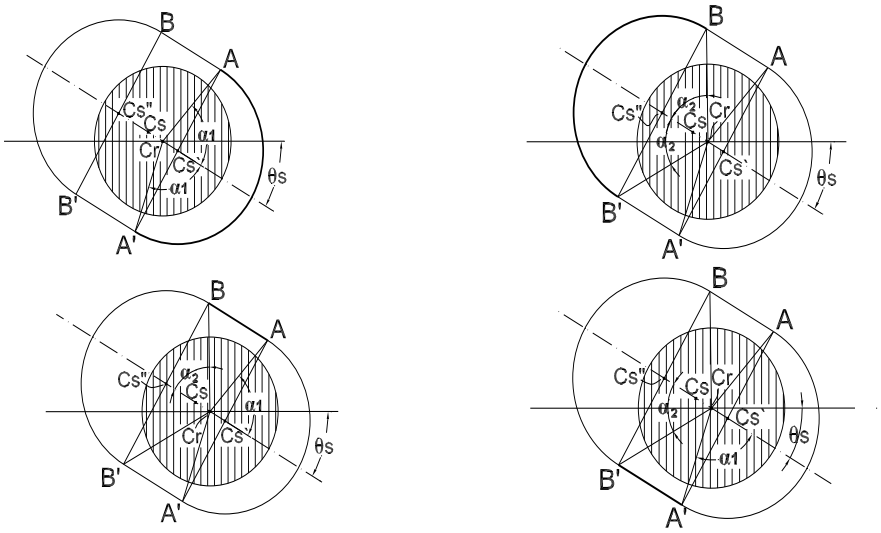

Figure 6. Each one of the four regions: I, II, III and IV respectively.

related part of the region and the θ's limit of each part, where A = $(\alpha 1 - \Theta_s)$; B = $(\pi - \Theta_s - \alpha 2)$; B' = $(\pi + \alpha 2 - \Theta_s)$; A' = $(2\pi - \alpha 1 - \Theta_s)$.

Table 1. The functions that describes the geometry of a singlelobe metal PCP.

Region	θ limits	Function —— $R_o(\theta, z)$
I	A' $\leq \theta <$ A	$(2E - d_{csr})\cos(\theta - \Theta_S) + \sqrt{R_s^2 - (2E - d_{csr})^2 \sin^2(\theta - \Theta_S)}$
II	B $\leq \theta <$ B'	$-(2E + d_{csr})\cos(\theta - \Theta_S) + \sqrt{R_s^2 - (2E + d_{csr})^2 \sin^2(\theta - \Theta_S)}$
III	A $\leq \theta <$ B	$\sqrt{R_s^2 + (2E - d_{csr})^2}\left[\frac{\sin\alpha_1}{\sin(\theta - \Theta_S)}\right]$
IV	B' $\leq \theta <$ A'	$-\sqrt{R_s^2 + (2E - d_{csr})^2}\left[\frac{\sin\alpha_1}{\sin(\theta - \Theta_S)}\right]$

2.2 Kinematic and Boundary Conditions

Note that the cross section of the rotor translates and rotates with respected to the center of the stator. The cross section of the PCP in four different times are shown in figure 4. To derive the appropriate boundary conditions, we need to determine the velocity of a point P in the rotor and of a point Q in the stator, as shown in figure 7.

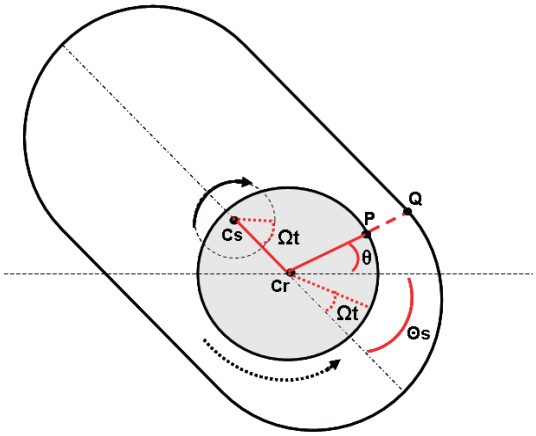

Figure 7. Variables to describe rotor's kinematic

The angular coordinate of P is $\theta = \gamma + \Omega t$, where γ is the inicial angle and Ω is the clockwise rotation. The position of the rotor's center (our center of reference) related to the stator's center is:
$X_{csr} = d_{csr}\cos(\Theta_s) = +2E\cos(\Omega t - \Theta_s)\cos(\Theta_s)$,
$Y_{csr} = -d_{csr}\sin(\Theta_s) = -2E\cos(\Omega t - \Theta_s)\sin(\Theta_s)$.

Thus the velocity of the rotor's center is: $\overrightarrow{V_{csr}} = \overrightarrow{V_{X_{csr}}} + \overrightarrow{V_{Y_{csr}}}$:
$\overrightarrow{V_{X_{csr}}} = -2e\Omega\sin(\Omega t - \Theta_s)\sin(\Theta_s)$, $\overrightarrow{V_{Y_{csr}}} = 2E\Omega\sin(\Omega t - \Theta_s)\cos(\Theta_s)$.

So, $(X_P, Y_P) = (X_{csr} + R_r\cos(\gamma + \Omega t), Y_{csr} + R_r\sin(\gamma + \Omega t))$ is the position of the point P related to the stator center and its velocity is $\overrightarrow{V_P} = \overrightarrow{V_{X_P}} + \overrightarrow{V_{Y_P}}$: $\overrightarrow{V_{X_P}} = V_{X_{csr}} - R_r\Omega\sin\theta$, $\overrightarrow{V_{Y_P}} = V_{Y_{csr}} + R_r\Omega\cos\theta$.

It is clear that the velocity of P related to our frame of reference, in the rotor center, is:
$\overrightarrow{V_{P_{csr}}} = (V_{X_P} - V_{X_{csr}},\ V_{Y_P} - V_{Y_{csr}}) = (-R_r\Omega\sin\theta,\ R_r\Omega\cos\theta)$.

Finally, the velocity of the point Q (located at the stator boundary), related to our coordinate system, is:
$\overrightarrow{V_{Qcsr}} = \overrightarrow{V_Q} - \overrightarrow{V_{csr}} \Rightarrow \overrightarrow{V_{Qcsr}} = -\overrightarrow{V_{csr}} = (2E\Omega\sin(\Omega t - \Theta_s)\cos(\Theta_s), -2E\Omega\sin(\Omega t - \Theta_s)\sin(\Theta_s))$, note that $\overrightarrow{V_Q} \equiv 0$, because the stator is stationary.

Applying the transformation matrix below, any vector can be written in cylindrical coordinates:

$$\begin{bmatrix} V_r \\ V_\theta \end{bmatrix} = \begin{bmatrix} \cos\theta & \sin\theta \\ -\sin\theta & \cos\theta \end{bmatrix} \begin{bmatrix} V_x \\ V_y \end{bmatrix}$$

Now, we are able to present all velocities in $r = R_o$ and $r = R_r$:

$$v(R_o) = V_{X_{Qcsr}}\cos\theta + V_{Y_{Qcsr}}\sin\theta = +2E\Omega\sin(\Omega t - \Theta_s)\cos(\Theta_s)$$
$$w(R_o) = -V_{X_{Qcsr}}\sin\theta + V_{Y_{Qcsr}}\cos\theta = -2E\Omega\sin(\Omega t - \Theta_s)\sin(\Theta_s)$$

$$v(R_r) = V_{X_{Pcsr}}\cos\theta + V_{Y_{Pcsr}}\sin\theta = 0 \qquad (3)$$

$$w(R_r) = -V_{X_{Pcsr}}\sin\theta + V_{Y_{Pcsr}}\cos\theta = \Omega R_r$$

It is clear that P rotates only and both, P and Q, do not have azimutal movement: $u(R_o) = u(R_r) = 0$.

Back to the equations (2) and applying the boundary conditions presented in equations (3), we are able to find

c_1, c_2, c_3, c_4 and write the complete expressions of u and w:

$$u = \left(\rho g - \frac{\partial p}{\partial z}\right)\frac{R_i^2}{4\mu}\left\{1 - \left(\frac{r}{R_i}\right)^2 + \left[\left(\frac{(R_o/R_i^2)-1}{\ln(R_o/R_i)}\right)\ln\left(\frac{r}{R_i}\right)\right]\right\} \tag{4}$$

$$w = \frac{\partial p}{\partial \theta}\frac{R_r}{2\mu}\left\{\frac{r}{R_r}\left[\ln(r) - \frac{1}{2} + \frac{r}{R_r}K - \frac{R_r}{r}\left(\ln(R_r) - \frac{1}{2} + K\right)\right]\right\} + \left(\frac{W_{Ro}R_o - \Omega R_r^2}{R_o^2 - R_r^2}\right)\left(r - \frac{R_r^2}{r}\right) + \Omega\frac{R_r^2}{r} \tag{5}$$

$$\text{where} \qquad \mathrm{K} = \frac{-\mathrm{R_o^2}\left(\ln \mathrm{R_o} - 1/2\right) + \mathrm{R_r^2}\left(\ln \mathrm{R_r} - 1/2\right)}{\mathrm{R_o^2} - \mathrm{R_r^2}}. \tag{6}$$

Up to this point, the pressure field is still unknown. In order to evaluate it, and since the expressions of u and w are known, the continuity equation can be integrated in the radius direction, from R_r to R_o:

$$\int_{R_r}^{R_o}\left\{\frac{\partial rv}{\partial r} + \frac{\partial w}{\partial \theta} + \frac{\partial ru}{\partial z}\right\}\mathrm{d}r = 0 \quad \Rightarrow \quad \underbrace{\int_{R_i}^{R_o}\frac{\partial rv}{\partial r}\,\mathrm{d}r}_{\mathrm{I}} + \underbrace{\int_{R_r}^{R_o}\frac{\partial w}{\partial \theta}\,\mathrm{d}r}_{\mathrm{II}} + \underbrace{\int_{R_r}^{R_o}\frac{\partial ru}{\partial z}\,\mathrm{d}r}_{\mathrm{III}} = 0 \tag{7}$$

where $\mathrm{I} = R_o v(R_o) - R_r v(R_r)$, $\mathrm{II} = \dfrac{\partial}{\partial\theta}\displaystyle\int_{R_r}^{R_o} w\,\mathrm{d}r - \left[w(R_o)\frac{\partial R_o}{\partial\theta} - w(R_r)\frac{\partial R_r}{\partial\theta}\right]$ and

$\mathrm{III} = \dfrac{\partial}{\partial z}\displaystyle\int_{R_r}^{R_o} ru\,\mathrm{d}r - \left[u(R_o)\frac{\partial R_o}{\partial z} - u(R_r)\frac{\partial R_r}{\partial z}\right]$

Applying the boundary conditions (3) in the equation (7), the continuity become:

$$\frac{\partial}{\partial z}\int_{R_r}^{R_o} ru\,\mathrm{d}r + \frac{\partial}{\partial\theta}\int_{R_r}^{R_o} w\,\mathrm{d}r - w(R_o)\frac{\partial R_o}{\partial\theta} - R_o v(R_o) = 0. \tag{8}$$

Using the known equations of the velocity field (eqs. (4) and (5)) to integrate w and ru in the radius direction:

$$\int_{R_r}^{R_o} w\,\mathrm{d}r = \frac{\partial p}{\partial\theta}\frac{R_r}{2\mu}\left\{\frac{1}{2R_r}\left[R_o^2\ln(R_o) - R_r^2\ln(R_r) - (R_o^2 - R_r^2)(1+K)\right] - R_r\left[\left(\ln(R_r) - \frac{1}{2} + K\right)\ln\left(\frac{R_o}{R_r}\right)\right]\right\}$$
$$+ \left(\frac{W_{R_o} + R_r^2}{R_o^2 - R_r^2}\right)\left[\frac{(R_o^2 - R_r^2)}{2} - R_r^2\ln\left(\frac{R_o}{R_r}\right)\right] - R_r^2\Omega\ln\left(\frac{R_o}{R_r}\right), \tag{9}$$

with K in equation (6),

$$\int_{R_r}^{R_o} ru\,\mathrm{d}r = \left(\frac{\partial \mathrm{p}}{\partial \mathrm{z}} - \rho\mathrm{g}\right)\left(\frac{-\mathrm{R_r^2}}{8\mu}\right)\left\{(\mathrm{R_o^2} - \mathrm{R_r^2})\left[1 - \left(\frac{\mathrm{R_o^2} - \mathrm{R_r^2}}{2\mathrm{R_r^2}}\right)\left(\frac{1}{\mathrm{R_r^2}\ln(\mathrm{R_o}/\mathrm{R_r})}\right)\left(\mathrm{R_o^2}\ln\left(\frac{\mathrm{R_o}}{\mathrm{R_r}}\right) - \frac{(\mathrm{R_o^2} - \mathrm{R_r^2})}{2}\right)\right]\right\}.$$

Finally, the equation can compactly be written as:

$$\frac{\partial}{\partial\theta}\left(C_1\frac{\partial p}{\partial\theta}\right) + \frac{\partial}{\partial z}\left(C_2\frac{\partial p}{\partial z}\right) = \frac{\partial}{\partial\theta}(C_{0W}) + \frac{\partial}{\partial z}(\rho g C_2) + w(R_o)\frac{\partial R_o}{\partial\theta} + R_o v(R_o); \tag{10}$$

where, $C_1 = \frac{R_r}{2\mu}\left\{\frac{1}{2R_r}\left[R_o^2\ln(R_o) - R_r^2\ln(R_r) - (R_o^2 - R_r^2)(1+K)\right] - R_r\left[\left(\ln(R_r) - \frac{1}{2} + K\right)\ln\left(\frac{R_o}{R_r}\right)\right]\right\}$

$C_2 = \left(\frac{-R_r^2}{8\mu}\right)\left\{(R_o^2 - R_r^2)\left[1 - \frac{(R_o^2 - R_r^2)}{2R_r^2} + \left(\frac{1}{R_r^2\ln(R_o/R_r)}\right)\left(R_o^2\ln\left(\frac{R_o}{R_r}\right) - \frac{(R_o^2 - R_r^2)}{2}\right)\right]\right\}$, and

$C_{0W} = -\left(\frac{W_{R_o}R_o - \Omega R_r^2}{R_o^2 - R_r^2}\right)\left[\frac{(R_o^2 - R_r^2)}{2} - R_r^2\ln\left(\frac{R_o}{R_r}\right)\right] - R_r^2\Omega\ln\left(\frac{R_o}{R_r}\right)$.

Note that K is the same used before (eq. (6)) and $\dfrac{\partial R_o}{\partial\theta}$ can be directly derived from the functions presented in table 1.

The equation (10) is a Poisson equation with the pressure field as unknown. The boundary conditions are: periodicity: $P(\theta = 0) = P(\theta = 2\pi)$; $\dfrac{\partial P}{\partial\theta}(\theta = 0) = \dfrac{\partial P}{\partial\theta}(\theta = 2\pi)$ and Dirichlet condition: $P(z = 0) = P_{in},\ P(z = L) = P_{out}$, for the suction and discharge of the pump.

This equation was discretized using a central finite difference and solved in the software matlab.

3. NUMERICAL RESULTS

In order to compare and validate our results we use the same pump, fluid and physical conditions as used by Olivet *et al*, [2] in their experimental study. The metal singlelobe PCP was chosen as the follow characteristics: pump length $L_b = 0.36$ m, length of each rotor pitch $L = 0.06$ m, number of the piches of the rotor $N_r = 6$, radius of the rotor's cross section $R_r = 0.02$ m, radius of the stator's cross section $R_s = 0.020185$ m, eccentricity $E = 0.004039$ m.

In these numerical experiments, the rotor velocity 300 rpm pumped a fluid of 42 cp against a differential of pressure of 345 kPa.

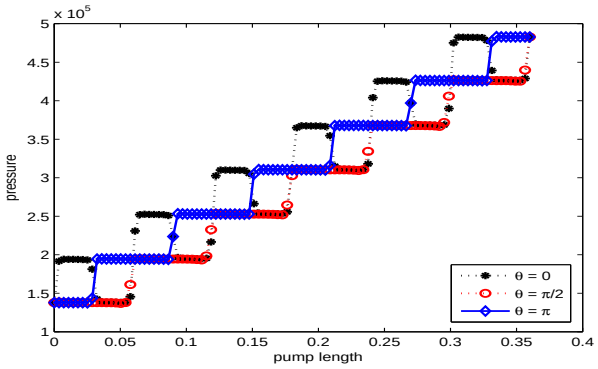

Figure 8. Pressure distribution along pump length

It is interesting that the model provides detailed information of the flow inside the pump. The obtained results were as expected, the relevant physical effects occur when the flow goes thought the gap, i.e. pump performance is defined by the flow between consecutives cavities. It can be seen in figure 8, which shows the pressure distribution along pump length for three different angles ($\theta = 0, \theta = \pi/2$ and $\theta = \pi$). Inside the cavity the pressure is almost constant and a large gradient occurs when the fluid flows through the clearance.

This phenomena can be also confirmed in figure 9. The left side of this figure shows the clearance and the right one the pressure distribution, both in a $\theta \times z$ plane and in the same moment. The first plots show the clearance and differential of pressure after 0.013 seconds and the second ones 0.150 seconds after, that is 3/4 of the pump rotation.

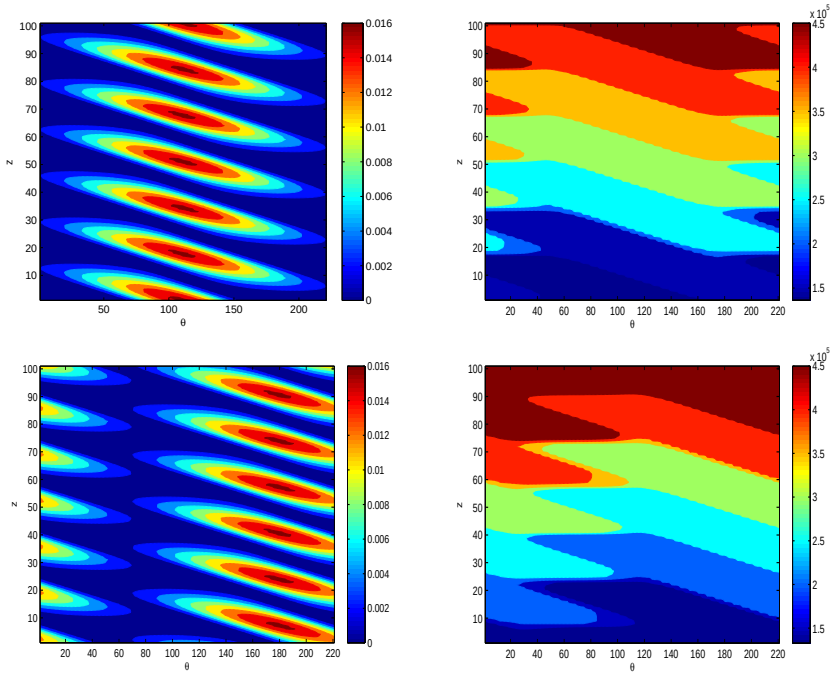

Figure 9. Clearance and pressure distribution in a $\theta \times z$ plane in two times: $t_1 = 0,013$s and $t_2 = 0,150$s .

The variation of the flow rate with time is presented in figure 10. Comparing two different imposed pressure's gradient, we can notice that the variation of the flow rate without differential of pressure ($\Delta P = 0$) is smooth and it loses this

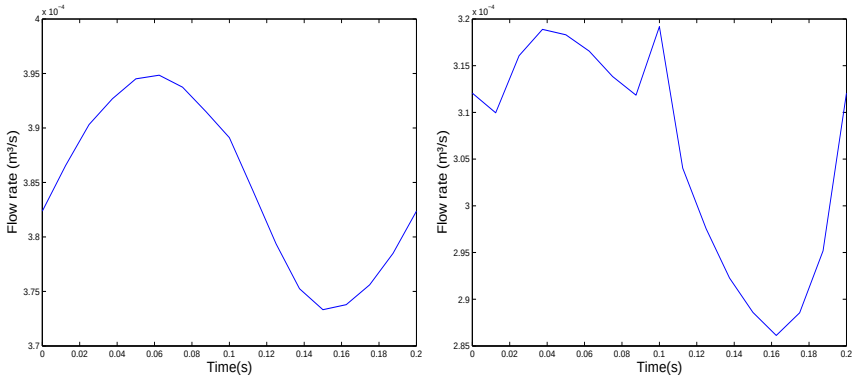

Figure 10. Flow rate versus time. $\Delta P = 0$, $\Delta P = 345kPa$.

smoothness when the imposed pressure's gradient increases ($\Delta P = 345kPa$). There are two peaks in the flow rate, one in the beginning and another in the middle of the pump cycle. The pump geometry suggest this variation in the flow rate. Notice in figure 4 that when the rotor is in the beginning and in the middle of one rotation it is located in the two extremes of the pump's cross section, touching the stator.

Once the pressure field is evaluated we can use the analytical expressions eq. (4) and eq. (5) to describe the velocity field. It is shown in a contour plot (fig. 11) of velocity and also of pressure, both in the same time and position ($t = 0.15$s and $z_1 = 0.036$m). The rotor squeeze the fluid to flow against the pressure gradient, and it is clear, analyzing the velocity field, the slippage, which is the responsible for the loss of efficiency in the pump. And we can also notice that the fluid recirculates. To compare our pump curve with an experimental data from Olivet *et al*, [2] and also with the numerical

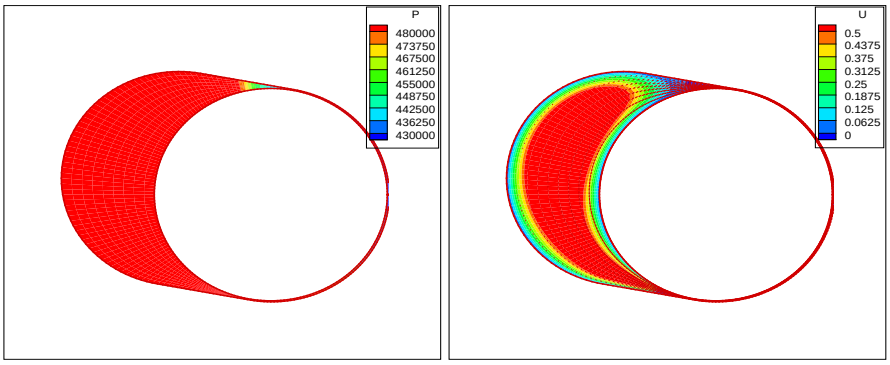

Figure 11. Contour graphic of pressure and velocity fields in the same position ($z_1 = 0.036$m) and time ($t_2 = 0.15$s).)

solution obtained with a commercial CFD software by (Paladino *et al*, 2008 [4]), a 300 rpm of rotor's velocity operating in a fluid with the viscosity, μ = 42cp were chosen. As shown in the comparative plot 12, our results agree well with the literature. The model can be used also to evaluate operational parameters of the pump. For example, the influence of the gap in the flow rate can be analyzed in the figure 13 . Defining a dimensionless flow rate as in equation 11 and varying the differential of pressure for three gaps.

$$Q_{\text{ad}} = \frac{Q_m}{[2 \cdot R_s \cdot E + \pi \cdot (R_s^2 - R_r^2)] \cdot (L/t)} \tag{11}$$

.

4. FINAL REMARKS

In this work, an asymptotic model for the flow inside a metallic (rigid) singlelobe progressive cavity pump was developed. The cross section is parameterized using cylindrical coordinates and there is no simplified assumption of the geometry and kinematics of the rotor. The proposed model reduces the three-dimensional transient Navier-Stokes equation to a quasi-steady state two-dimensional Poisson's equation for the pressure field and provide detailed information about the flow inside the pump. The resulting 2D equation for the pressure field at each time step was discretized with a second order finite difference approximation. The model was used to obtain predictions of the pump performance curve as a function of rotor speed, liquid properties and pump geometry. The results obtained agree very well with experimental

datas and with the complete 3D model and the computational time required was order of magnitude smaller. Another interesting characteristic of this asymptotic model is that it can be easily extended to PCPs with deformable stator, different geometries and also multiphase flows. And also, because of the more efficient computation, the model can be included into a PCP simulator to provide the pump curve at any operational conditions.

5. REFERENCES

Moineau R., 1930, "A new capsulism", Doctoral Thesis.

Olivet A., Gamboa J.A. and Kenvery F., 2002, "Experimental Study of Two-Phase Pumping in a Progressing Cavity Pump Metal to Metal", Society of Petroleum Engineers SPE, Vol. 77730.

Olivet A. and Gamboa J.A., 2003, "New Approach for Modelling Progressive Cavity Pumps Performance", Society of Petroleum Engineers - SPE, Vol. 84137.

Paladino E., Lima J.A. and Almeida R.F.C.,2008, "Computing Modeling of the Three-Dimensional Flow in a Metallic Stator Progressing Cavity Pump", Society of Petroleum Engineers - SPE, Vol. 114110.

Li Y., Hsieh F. 1996, "Modeling of flow in a single screw struder", Journal of Food Engineering, Vol. 27(4), pp.353-375.

Suresh A., Chakraborty S., Kargupta K., Ganguly S. 2008, "Low-dimensional models for describing mixing effects in reactive extrusion of polypropylene", Chemical Engineering Science, Vol. 63(14), pp. 3788-3801

Carvalho M.S. and Pina E.,2006, "Three-Dimensional Flow of a Newtonian Liquid Through an Annular Space with Axially Varying Eccentricity", Jounal of Fluids Engineering, Vol.128, pp. 226-230.

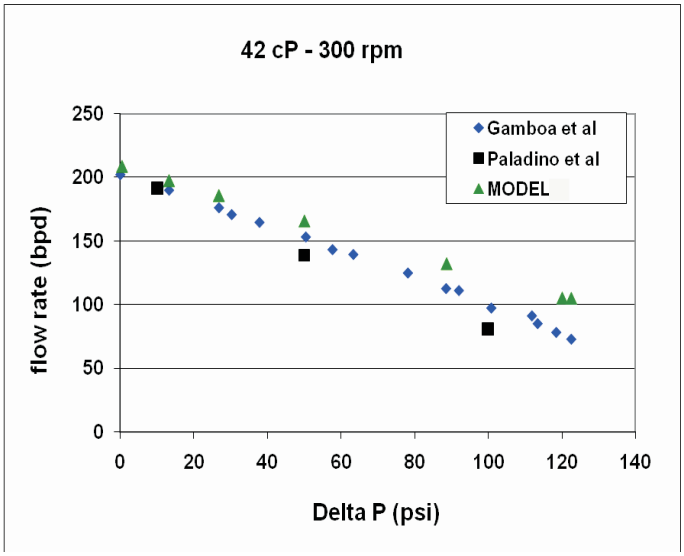

Figure 12. μ = 42cP, rotor velocity 300 rpm

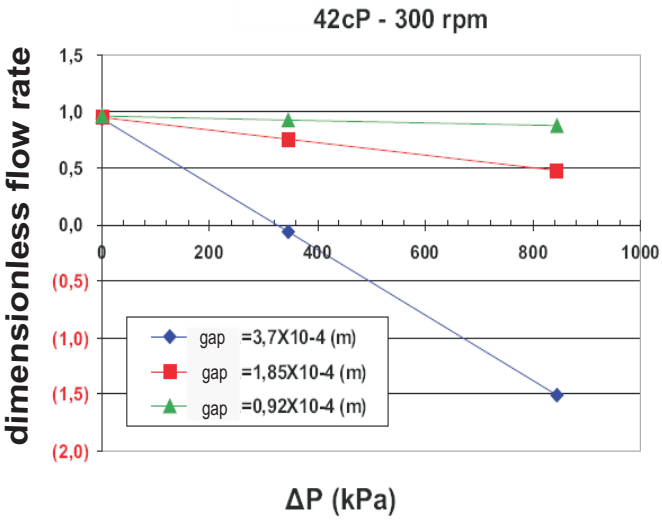

Figure 13. $Q_a \times \Delta P$, three different gaps